

Comparative proteomic analysis of two *Entamoeba histolytica* strains with different virulence phenotypes identifies peroxiredoxin as an important component of amoebic virulence

Paul H. Davis,^{1,2} Xiaochun Zhang,¹ Jianhua Guo,¹
R. Reid Townsend¹ and Samuel L. Stanley, Jr^{1,2*}

¹Department of Medicine, Washington University School of Medicine, St Louis, MO, USA.

²Department of Molecular Microbiology, Washington University School of Medicine, St Louis, MO, USA.

Summary

Entamoeba histolytica is a protozoan intestinal parasite that causes amoebic colitis and amoebic liver abscess. To identify virulence factors of *E. histolytica*, we first defined the phenotypes of two *E. histolytica* strains, HM-1:IMSS, the prototype virulent strain, and *E. histolytica* Rahman, a strain that was reportedly less virulent than HM-1:IMSS. We found that compared with HM-1:IMSS, Rahman has a defect in erythrophagocytosis and the ability to cause amoebic colitis in human colonic xenografts. We used differential in-gel 2D electrophoresis to compare the proteome of Rahman and HM-1:IMSS, and identified six proteins that were differentially expressed above a fivefold level between the two organisms. These included two proteins with antioxidative properties (peroxiredoxin and superoxide dismutase), and three proteins of unknown function, grainin 1, grainin 2 and a protein containing a LIM-domain. Overexpression of peroxiredoxin in Rahman rendered the transgenic trophozoites more resistant to killing by H₂O₂ *in vitro*, and infection with Rahman trophozoites expressing higher levels of peroxiredoxin was associated with higher levels of intestinal inflammation in human colonic xenografts, and more severe disease based on histology. In contrast, higher levels of grainin appear to be associated with a reduced virulence phenotype, and *E. histolytica* HM-1:IMSS trophozoites infecting human intestinal xenografts show marked decreases in grainin expression. Our data indicate that there are definable molecular differences between Rahman and HM-1:IMSS that may explain the

phenotypic differences, and identify peroxiredoxin as an important component of virulence in amoebic colitis.

Introduction

Entamoeba histolytica infection remains a critical threat to health in much of the world. *E. histolytica* trophozoites can penetrate and inflame the colonic mucosa, causing amoebic colitis, and spread through the portal circulation to the liver, where they cause amoebic liver abscess (Stanley, 2003). However, it has been observed that infection with *E. histolytica* does not always result in disease. Possible explanations for this phenomenon include host immunity, host nutritional status, the gut microbiota, and genetic differences between *E. histolytica* isolates. *E. histolytica* strain Rahman was isolated from an asymptomatic patient in 1972 (Diamond *et al.*, 1978; Mattern *et al.*, 1978). Based on the nucleotide sequence of its 5.8 s rRNA, Rahman is *E. histolytica*, yet in various *in vitro* assays it appears to be less virulent than the prototype *E. histolytica* HM-1:IMSS strain (Moody *et al.*, 1998; Som *et al.*, 2000; Bujanover *et al.*, 2003). The availability of Rahman, and the virulent HM-1:IMSS strain of *E. histolytica*, provides a powerful tool for identifying virulence factors of *E. histolytica*. Here we report the use of comparative proteomics of *E. histolytica* HM-1:IMSS and *E. histolytica* Rahman to identify virulence factors. To ensure that we were truly comparing phenotypically distinct organisms, we performed both *in vitro* and *in vivo* studies of each strain used in this comparison, and show for the first time that Rahman has a defect in erythrophagocytosis and a significant defect in the ability to cause amoebic colitis in human colonic xenografts. With these phenotypically defined strains, we have used differential in-gel 2D electrophoresis (DIGE) to compare the proteome of Rahman and HM-1:IMSS. The proteomic comparison revealed differential levels of two molecules linked to resistance of host oxidative defences, peroxiredoxin, and superoxide dismutase (SOD), and three proteins of unknown function, including grainins 1 and 2. We report here that transgenic Rahman trophozoites expressing higher levels of peroxiredoxin cause greater

Accepted 19 July, 2006. *For correspondence. E-mail sstanley@id.wustl.edu; Tel. (+1) 314 2860432; Fax (+1) 314 3623525.

inflammatory responses and damage to human colonic xenografts, consistent with a potential role for peroxidase in *E. histolytica* virulence.

Results and discussion

Rahman shows decreased phagocytic activity in vitro

We felt it was critical to define the virulence phenotype of each of the *E. histolytica* strains before beginning proteomic comparisons. Previous studies have demonstrated that Rahman is less effective at damaging mammalian cell monolayers and has reduced cytopathic effects, but differences between *E. histolytica* HM-1:IMSS and Rahman in phagocytosis or resistance to oxidative stress have not been definitely established. (Moody *et al.*, 1998; Leroy *et al.*, 2000; Bujanover *et al.*, 2003; Dvorak *et al.*, 2003; Lauwaet *et al.*, 2004).

Genetically engineered or mutant *E. histolytica* that are defective in phagocytosis show decreased virulence (Orozco *et al.*, 1985; Rodriguez and Orozco, 1986; Marion *et al.*, 2004). We compared the ability of *E. histolytica* HM-1:IMSS and Rahman to bind and phagocytose human erythrocytes. Using an assay that photometrically measures red blood cell uptake, we found that after 15 min, *E. histolytica* HM-1:IMSS trophozoites ingested 2.9-fold more erythrocytes than *E. histolytica* Rahman ($P < 0.05$), consistent with a phagocytic defect in Rahman. In a previous study, a trend towards reduced erythrophagocytosis by Rahman compared with HM-1:IMSS was observed, but this did not obtain statistical significance (Bujanover *et al.*, 2003). One explanation for this discrepancy may be that our animal-passaged and highly virulent HM-1:IMSS strain may have greater phagocytic capacity than the HM-1:IMSS strain used in the prior work.

Rahman does not cause tissue damage in human colonic xenografts in the SCID-HU-INT model of disease

Others have shown that *E. histolytica* strain Rahman shows reduced virulence in rodent models of amoebic liver abscess, but no prior studies have looked at its ability to cause amoebic colitis (Mattern *et al.*, 1978; Burchard and Mirelman, 1988). We used severe combined immunodeficient mice implanted with human colonic xenografts (SCID-HU-INT mice) to compare infection between *E. histolytica* HM-1:IMSS and Rahman (Seydel *et al.*, 1997; 1998; Davis and Stanley, 2003). Approximately 20 h following direct inoculation of *E. histolytica* Rahman or HM-1:IMSS trophozoites into the lumen of the colonic xenografts, fluoresceinated dextran was introduced into the lumen of the human colonic xenograft. Four hours later, mice were sacrificed and the extent of colonic

disease quantified by measuring the levels of myeloperoxidase (MPO) within the graft (as a marker for neutrophil influx and inflammation) and fluoresceinated dextran in the serum of the mouse (as a marker for damage to the intestinal permeability barrier). As shown in Fig. 1, infection with *E. histolytica* HM-1:IMSS was associated with a marked influx of neutrophils into the human colonic xenograft, while there were significantly lower mean MPO levels ($P < 0.05$) in human colonic xenografts infected with *E. histolytica* Rahman. The MPO value for Rahman was higher than that seen for sham-infected grafts, suggesting that Rahman does induce a low level host inflammatory response, and we could detect some inflammatory cells in histologic sections from human colonic xenografts infected with Rahman (data not shown).

Colonic infection with *E. histolytica* Rahman did not cause marked damage to the intestinal permeability barrier. As shown in Fig. 1, there was no significant difference in the mean level of FITC-dextran in the serum of SCID-HU-INT mice that had been infected with Rahman compared with SCID-HU-INT mice undergoing sham (media only) inoculation. In contrast, infection of the human intestinal xenografts with *E. histolytica* HM-1:IMSS damaged the intestinal permeability barrier, resulting in significantly ($P < 0.05$ compared with Rahman-infected human colonic xenografts) higher levels of FITC-dextran in the serum of SCID-HU-INT mice. These data suggest that Rahman is significantly less virulent than *E. histolytica* HM-1:IMSS in this model of amoebic colitis.

Proteomic comparison of E. histolytica HM-1:IMSS and E. histolytica Rahman using DIGE

We used 2-dimensional differential in-gel electrophoresis (2D-DIGE) to compare the proteomes of *E. histolytica* Rahman and *E. histolytica* HM-1:IMSS. We were able to resolve an average of 2595 spots (± 159 spots) in three 2-D gels each containing distinct biological replicates of lysates from strain Rahman and HM-1:IMSS. The number of differentially expressed spots was a function of the cut-off used for differential expression, but requiring a minimum of fivefold differential expression yielded an average of 20 (± 5) spots expressed at a higher level in *E. histolytica* HM-1:IMSS than Rahman, with an average of 20 (± 2) spots showing the opposite pattern. Figure 2 is an image of one representative gel. Using the strictest criteria (fivefold or greater difference in intensity, reproducibly identified in two separate DIGE runs with biological replicates) we found six proteins that could be unequivocally identified that showed differential expression between Rahman and HM-1:IMSS.

Three proteins were present at higher levels in HM-1:IMSS, and three at higher levels in Rahman. One of the proteins expressed at higher levels in HM-1:IMSS was

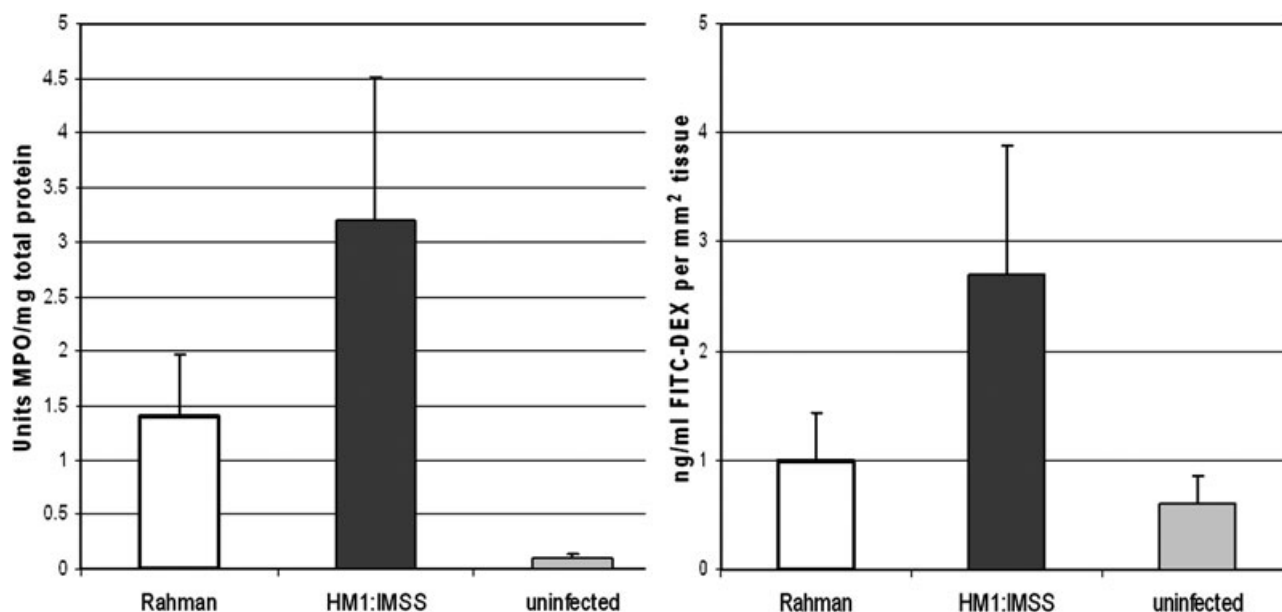


Fig. 1. *E. histolytica* Rahman shows markedly reduced virulence compared with HM-1:IMSS in the SCID-HU-INT model of amoebic colitis. Left panel. Mean MPO levels in *E. histolytica* Rahman-infected human colonic xenografts ($n = 12$) are significantly lower than those seen in human colonic xenografts infected with *E. histolytica*-HM-1:IMSS ($n = 10$) ($P < 0.05$).

Right panel. In the same animals, mean serum levels of FITC-dextran are significantly lower in SCID-HU-INT mice after Rahman-infection of the human colonic xenografts (showing less damage to the intestinal permeability barrier) compared with SCID-HU-INT mice with human colonic xenografts infected with wild-type *E. histolytica* HM-1:IMSS trophozoites ($P < 0.05$).

a LIM-domain protein (gi56474157). The LIM domain is a cysteine and histidine-rich, zinc-co-ordinating domain composed of two zinc fingers. LIM domains mediate protein–DNA, or more often, protein–protein interactions (Kadmas and Beckerle, 2004). LIM domains are found in eukaryotes within proteins involved in regulating transcription, cell lineage specification, and cytoskeletal organization. The function of the *E. histolytica* LIM protein, and whether it is likely to have any role in virulence, is unknown.

The second protein found at higher levels in *E. histolytica* HM-1:IMSS than *E. histolytica* Rahman is alcohol dehydrogenase 3 (gi67468848). In separate studies, we have confirmed the differential expression of ADH3 between *E. histolytica* HM-1:IMSS and other *Entamoeba* species/strains, and explored its potential role in virulence (P.H. Davis, *et al.*, in preparation).

Peroxiredoxin, a surface molecule shown *in vitro* to protect against such ROS as H_2O_2 , was shown to be higher in HM-1 than Rahman (gi56469992). Previous work has shown that this protein can degrade H_2O_2 effectively (Bruchhaus *et al.*, 1997). It has been proposed by Choi *et al.* that peroxiredoxin may play a role in counteracting ROS and NOS attacks employed by inflammatory host cells. They observed that peroxiredoxin levels are significantly higher in *E. histolytica* than *Entamoeba dispar*, a non-pathogenic commensal species that is morphologically identical to *E. histolytica* (Choi *et al.*, 2005).

More recently, a transcriptional comparison of *E. histolytica* HM-1:IMSS compared with the commensal *E. dispar* and *E. histolytica* Rahman noted 2.4-fold and 1.5-fold more peroxiredoxin transcript in HM-1:IMSS respectively (MacFarlane and Singh, 2006).

If peroxiredoxin expression is required for *E. histolytica* survival within the host, one might see increased expression of peroxiredoxin in *E. histolytica* trophozoites obtained from host tissue. We used real-time PCR to measure the transcript levels for peroxiredoxin in *E. histolytica* HM-1:IMSS trophozoites present within human colonic xenografts and compared the peroxiredoxin transcript levels with cultured *E. histolytica* trophozoites. As shown in Fig. 3, we saw no significant difference in transcript levels at 4 or 12 h after infection, but did see a greater than eightfold increase in peroxiredoxin expression in *E. histolytica* HM-1:IMSS trophozoites present in human intestinal xenografts for 24 h. This is particularly interesting, because our previous studies suggest that host inflammatory responses are maximal at 24 h after colonic infection in the SCID-HU-INT model (Seydel *et al.*, 1998), suggesting that amoebic peroxiredoxin levels could increase in response to the presence of host inflammatory cells.

We found that SOD was present at a higher level in Rahman than in HM-1:IMSS (gi56465110). This was unexpected, as SOD could be hypothesized to be a virulence factor, based on a possible role in resistance to

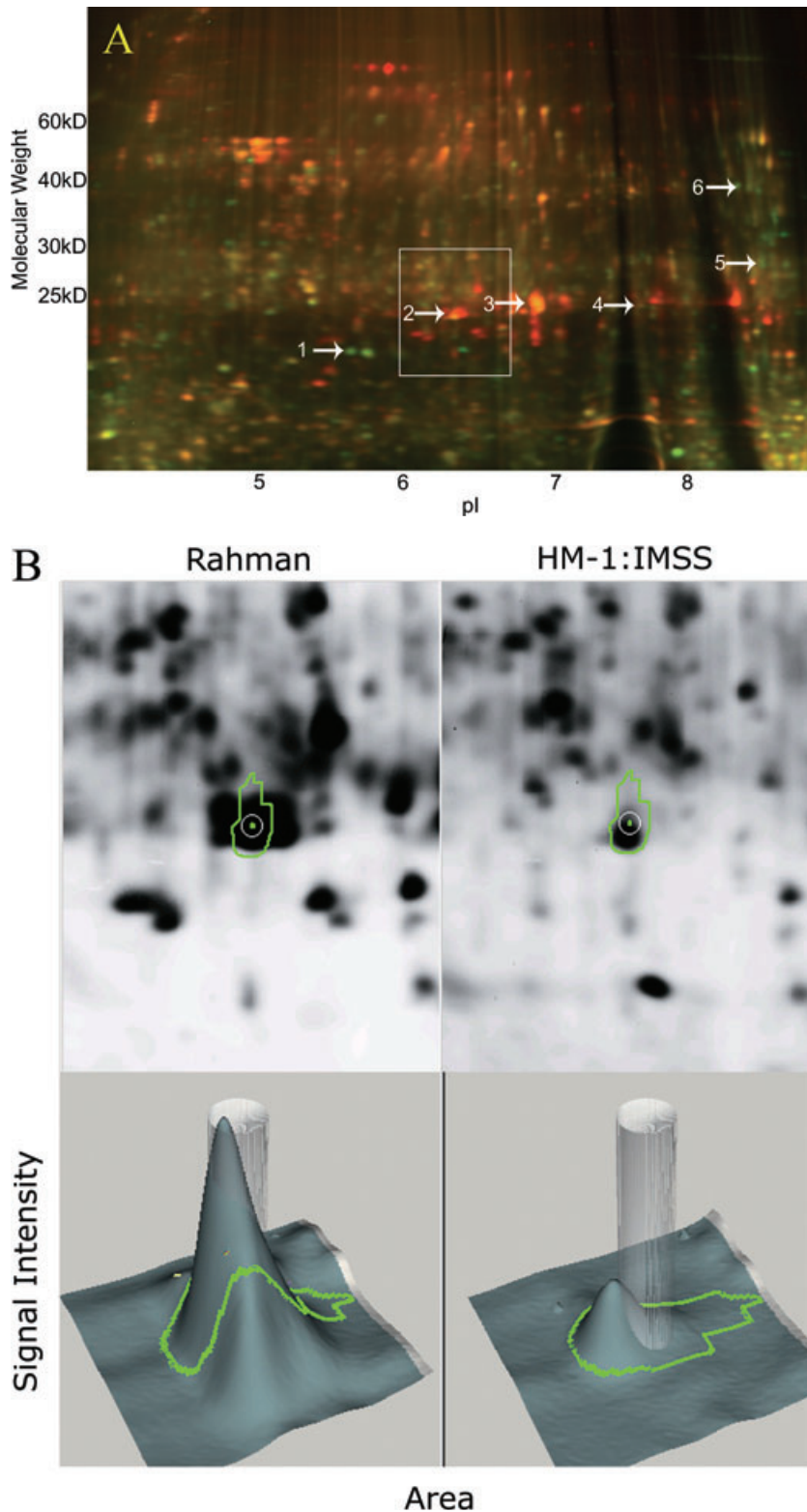


Fig. 2. Differential in-gel 2D electrophoresis of *E. histolytica* Rahman versus HM-1:IMSS. A. Two colour image of one of the Rahman versus HM-1 DIGE gels used for this analysis. 2754 distinct fluorescent spots were computationally observed; 20 were > fivefold higher in HM-1:IMSS compared with Rahman, and 19 were fivefold lower in HM-1:IMSS compared with Rahman. Increasing green represents greater expression in HM-1:IMSS, increasing red represents higher expression in Rahman overabundance. Yellow indicates similar protein level. Numbered arrows represent the following proteins, with their calculated molecular weight and isoelectric point as computed from the full protein sequence using ScanSite (http://scansite.mit.edu/calc_mw_pi.html): (1) LIM-domain protein: 16 kDa, pI 5.4; (2) grainin 1: 24 kDa, pI 6.3; (3) SOD: 22 kDa, pI 6.3; (4) grainin 2: 24 kDa, pI 8.4; (5) peroxiredoxin: 27 kDa, pI 8.2; (6) alcohol dehydrogenase 3: 42 kDa, pI 6.6. The box outlines the area found in (B). B. The gel area and spot representing grainin 1. The top panel is a fluorescent intensity scan of strain Rahman; the comparable region from HM-1:IMSS is on the right. The spot was identified as grainin 1 by mass spectroscopy. Below, each panel represents the 3D intensity plots from that gel using Decyder software. The region demarcated in green was used to calculate the volume fold difference between the strains' grainin 1 protein, which was 5.31-fold higher in *E. histolytica* Rahman than *E. histolytica* HM-1:IMSS in this gel. The transparent grey vertical column indicates the gel plug picking location.

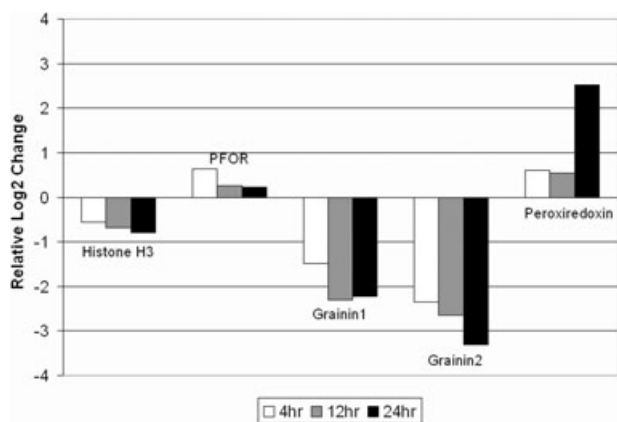


Fig. 3. Quantitative real-time PCR assay demonstrates a decrease in the expression of the genes encoding grainins 1 and 2 and increase in peroxiredoxin when *E. histolytica* trophozoites are within human intestinal xenografts. Transcript levels were measured in mRNA from human intestinal xenografts at 4, 12 and 24 h after infection with 1×10^6 *E. histolytica* HM-1:IMSS trophozoites and compared with levels in mRNA obtained from *E. histolytica* HM-1:IMSS trophozoites grown in log phase culture. PFOR, pyruvate ferredoxin : oxidoreductase.

reactive oxygen intermediates produced either by host phagocytic cells or those present in the higher oxygen environment associated with invasion into the colonic mucosa (Akbar *et al.*, 2004). Increased expression of SOD has been linked to the development of low level metronidazole resistance in *E. histolytica* trophozoites, and it would be of interest to determine whether Rahman shows greater inherent resistance to metronidazole than HM-1:IMSS (Samarawickrema *et al.*, 1997; Wassmann *et al.*, 1999).

The novel proteins grainin 1 (gi5813875) and grainin 2 (gi56466988) were also expressed at higher levels in Rahman than in HM-1:IMSS (Fig. 2). Grainins are calcium binding proteins of unknown function found in *E. histolytica* granules (Nickel *et al.*, 2000). Intriguingly, Bruchhaus *et al.* using differential display PCR reported that *E. histolytica* HM-1:IMSS trophozoites recently isolated from amoebic liver abscesses showed lower levels of grainin 1 gene expression than HM-1:IMSS trophozoites in long-term culture (Bruchhaus *et al.*, 2002). This finding was consistent with the possibility that grainin expression is associated with reduced virulence, and may serve as a marker for decreased pathogenic potential.

If grainin expression is associated with reduced virulence, then grainin gene expression might decrease under other conditions where *E. histolytica* HM-1:IMSS is invading into host tissue. To explore this possibility, we measured the transcription of the grainin 1 and 2 genes in *E. histolytica* trophozoites that were obtained from amoebic colitis lesions in human intestinal xenografts. As shown in Fig. 3, using real-time PCR on RNA obtained from human intestinal xenografts infected with *E. his-*

tolytica HM-1:IMSS trophozoites at 4, 12 and 24 h, compared with RNA obtained from trophozoites grown under standard culture conditions, we found a 3- to 10-fold decrease in grainin gene expression in trophozoites present in human intestinal xenografts. In contrast, no change in the expression of the genes encoding *E. histolytica* histone H3 or *E. histolytica* pyruvate ferredoxin : oxidoreductase were seen. These data, along with recently published results indicating that grainin expression is decreased in *E. histolytica* HM-1:IMSS trophozoites isolated from mouse colon (Gilchrist *et al.*, 2006), provide additional support for the concept of an inverse relationship between grainin levels and virulence.

It should be noted that another known molecular difference between strain Rahman and strain HM-1:IMSS is the structure of the GPI-anchored proteophosphoglycans (PPGs), which comprise the major surface glycocoat of the trophozoite (Moody-Haupt *et al.*, 2000). However, we were unable to detect any differences in either enzymes associated with GPI synthesis or possible peptide components between the two strains in our assay.

Overexpression of peroxiredoxin in E. histolytica Rahman confers increased resistance to oxidative stress, and increases virulence in the SCID-HU-INT model of amoebic colitis

To determine whether the lower levels of peroxiredoxin we found in *E. histolytica* Rahman may contribute to its reduced virulence, we used episomal expression of the peroxiredoxin gene to increase peroxiredoxin levels in Rahman. Expression of the plasmid pNeoPRD (Wassmann *et al.*, 1999) in Rahman led to peroxiredoxin levels that were 7.7 times that seen in non-transfected Rahman based on densitometry (Fig. 4). This finding was confirmed by immunofluorescence studies which showed increased intensity of staining for peroxiredoxin in Rahman transfected with pNeoPRD compared with wild-type Rahman trophozoites, with similar (primarily surface labelling) staining patterns (data not shown) compared with HM-1:IMSS.

We first examined whether increased peroxiredoxin levels in Rahman would increase its resistance to oxidative stress. As shown in Fig. 5, *E. histolytica* Rahman trophozoites expressing pNeoPRD showed higher survival after H_2O_2 exposure than wild-type Rahman trophozoites, and now became comparable to *E. histolytica* HM-1:IMSS trophozoites. These results indicate that peroxiredoxin plays a direct role in mediating resistance to H_2O_2 in Rahman.

To assess whether overexpression of peroxiredoxin would alter the virulence of *E. histolytica* Rahman, we infected human intestinal xenografts in SCID-HU-INT mice with either wild-type *E. histolytica* Rahman or

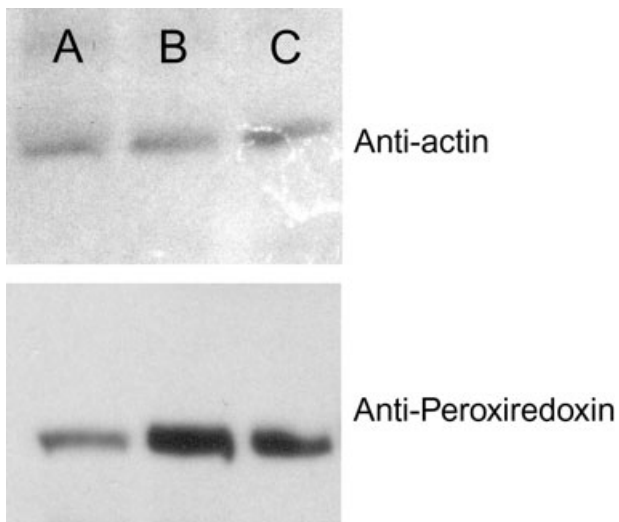


Fig. 4. Overexpression of peroxiredoxin in *E. histolytica* Rahman transfected with pNeoPRD. Lysates from non-transfected *E. histolytica* Rahman (A), *E. histolytica* Rahman transfected with pNeoPRD (B), and *E. histolytica* strain HM-1:IMSS (C) were separated by SDS-PAGE and immunoblotted with anti-peroxiredoxin or anti-actin antibodies.

Rahman expressing pNeoPRD. Among 12 human intestinal xenografts infected with Rahman only one showed visible tissue damage in a histological section (Fig. 6A). While trophozoites are clearly visible, and evidence for some invasion was present, no marked inflammatory response was seen. Histological examination of 12 human intestinal xenografts infected with Rahman pNeoPRD showed that four of 12 grafts had visible disease with invading trophozoites and marked inflammation present (see Fig. 6B and C for two representative xenografts). Measurements of MPO were consistent with the histologic findings and showed statistically significant higher ($P = 0.03$, $n = 12$) mean level of MPO in human intestinal xenografts infected with Rahman pNeoPRD (2.64 units mg^{-1} protein) than wild-type *E. histolytica* Rahman trophozoites (1.40 units mg^{-1} protein). We did not detect a statistically significant difference in FITC levels between the two groups (data not shown). This is not necessarily unexpected given the total absence of disease seen in eight of 12 of the Rahman pNeoPRD infected xenografts. Taken together, these data indicate that increased expression of peroxiredoxin in *E. histolytica* Rahman trophozoites appears to increase their virulence. Whether this is related directly to peroxiredoxin conferring a greater resistance to host reactive oxygen defences, or another mechanism remains unknown.

In summary, our phenotypic and proteomic comparisons identified a number of differences between the virulent *E. histolytica* HM-1:IMSS strain and the *E. histolytica* Rahman strain. Rahman shows increased expression of the grainin proteins, which appear to be associated with

reduced virulence, and lower levels of peroxiredoxin compared with HM-1:IMSS. Increasing peroxiredoxin levels in Rahman trophozoites renders them more resistant to reactive oxygen intermediates than wild-type Rahman, and increases their virulence in our model of amoebic colitis. Given the scope of the differences between Rahman and HM-1:IMSS in phagocytosis, cytopathic effects, resistance to H_2O_2 , and the ability to cause disease in animal models of amoebic liver abscess and amoebic colitis, it seems unlikely that a single or even a few gene products will explain all of the differences between the two strains. However, our success in identifying and validating new targets suggests that comparative proteomics may be a useful approach in defining physiologically relevant differences between *E. histolytica* HM-1:IMSS and Rahman.

Experimental procedures

Entamoeba strains

Our laboratory strain of *E. histolytica* HM-1:IMSS was originally obtained from ATCC, but has been passaged multiple times through animal livers to maintain virulence. Strain *E. histolytica* Rahman was obtained from ATCC, #50738. Transfectant R-pNeoPRD was created by transfecting plasmid pNeoPRD (Wassmann *et al.*, 1999) into strain Rahman. Transfection was performed similarly as previously described (Hamann *et al.*, 1995). Amoeba were chilled on ice for 10 min, spun at 400 g for 5 min and counted by haemocytometer. Volumes were adjusted to yield 1×10^6 amoeba ml^{-1} , which were washed $2 \times$ with cold PBS,

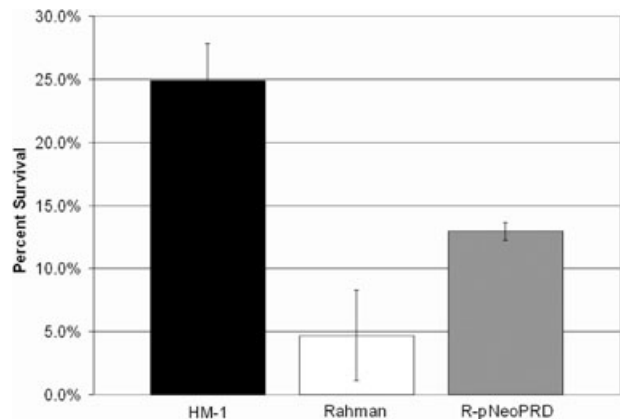


Fig. 5. Overexpression of *E. histolytica* peroxiredoxin confers protection against H_2O_2 . Trypan blue staining was used to measure the percentage of either *E. histolytica* HM-1:IMSS, *E. histolytica* Rahman, or Rahman expressing pNeoPRD (R-pNeoPRD) trophozoites remaining viable following 1 h exposure to 5 mM H_2O_2 at 37°C. Results are the means for four separate experiments. Overexpression of pNeoPRD rendered Rahman equivalent in resistance to HM-1:IMSS ($P = 0.68$ for the difference between them). Both R-pNeoPRD ($P = 0.05$) and HM-1:IMSS ($P < 0.01$) trophozoites were significantly more resistant to H_2O_2 than Rahman trophozoites.

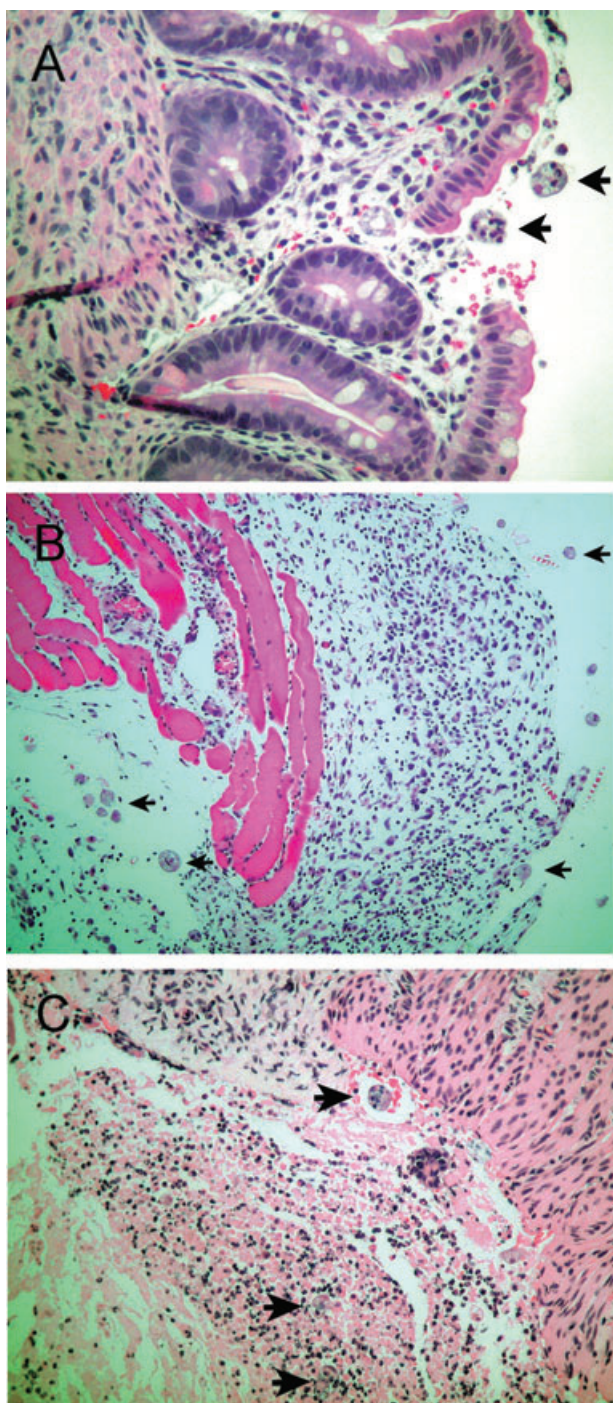


Fig. 6. *E. histolytica* Rahman transfected with pNeoPRD show greater invasion of host tissue than wild-type *E. histolytica* Rahman in human intestinal xenografts with histologically visible infection.

A. Section of a human intestinal xenograft showing *E. histolytica* Rahman trophozoites (arrows) near a small area of mucosal disruption and haemorrhage 24 h after infection. No marked inflammatory response is visible. This was the only human intestinal xenograft infected with Rahman where *E. histolytica* trophozoites were visible. Magnification 200 \times .

B. Section of a human intestinal xenograft obtained 24 h after infection with *E. histolytica* Rahman trophozoites (arrows) transfected with pNeoPRD. Note the nearly total disruption of the mucosal architecture and invasion into the submucosal surface. Magnification 100 \times .

C. Section from another human intestinal xenograft infected with *E. histolytica* Rahman trophozoites (arrows) transfected with pNeoPRD. There is significant destruction of the mucosal architecture and a marked neutrophilic infiltrate is present. Magnification 150 \times .

R-pNeoPRD was maintained at 40 $\mu\text{g ml}^{-1}$ G418 prior to experimental use.

SCID-HU-INT model of amoebic colitis

Severe combined immunodeficient mice were engrafted in the subscapular region with human colonic xenografts as previously described (Seydel *et al.*, 1998). Grafts were infected with an intraluminal inoculation of 1×10^6 trophozoites of *E. histolytica* HM-1:IMSS, Rahman, or Rahman transfected with pNeoPRD, and infection was assessed 24 h later. To measure the integrity of the intestinal permeability barrier, 20 h after infection human intestinal xenografts were intraluminally inoculated with fluoresceinated dextran, and serum levels of fluoresceinated dextran were measured using a fluorescent plate reader 4 h later (Seydel *et al.*, 1998). Grafts were removed at the time of sacrifice, and levels of MPO (as a marker for the influx of inflammatory cells into the graft) were measured according to our previously described assay (Seydel *et al.*, 1998). For histologic analysis, sections of the human intestinal xenograft were fixed in formalin, sectioned and stained with haematoxylin and eosin as previously described (Seydel *et al.*, 1997).

Erythrophagocytosis assay

Erythrophagocytosis experiments were carried out as described in Marion *et al.* (2004). Briefly, human donor O+ RBCs were collected and washed 2 \times with cold amoeba media and resuspended to 2×10^9 cells ml^{-1} . Amoeba were chilled on ice for 5 min, spun and counted with a haemocytometer, then warm media were used to volume-adjust the pellet to result in 2×10^6 amoeba ml^{-1} . RBC and amoeba were mixed 100:1 and incubated for 15 min at 37 $^{\circ}\text{C}$. The mixture was then washed 3 \times with ddH₂O, then 1 \times cold PBS. The pellet was dissolved in 0.5 ml concentrated formic acid, transferred to a cuvette, and the resulting solution was measured for absorbance at 400 nm using a spectrophotometer.

Differential in-gel 2D electrophoresis

For DIGE comparison, approximately 1×10^6 HM-1:IMSS or Rahman trophozoites were harvested simultaneously from

and once with cold, fresh cytomix. The amoeba were finally resuspended with 800 μl cytomix and 60 μg DNA (stored at ~ 1 mg DNA ml^{-1} water) into a chilled 0.4 cm electroporation cuvette. A Bio-Rad GenePulser XCell was set to 25 μF and 3000 V cm^{-1} . Two successive pulses were completed 30 s apart without disturbing the cuvette yielding a time constant of 0.4 ms, then amoeba were immediately placed in amoeba media and grown for 72 h before G418 drug selection was started at 2 $\mu\text{g ml}^{-1}$. All were maintained in culture medium BI-S-33 as previously described (Li *et al.*, 1988), and

culture via chilling at 4°C for 5 min. Amoeba were washed three times in ice-cold PBS, lysed in lysis buffer formulated to minimize post-lysis proteolysis (7 M Urea, 2 M thiourea, 4% CHAPS, 30 mM Tris, 5 mM magnesium acetate, 1× Roche Complete protease inhibitor cocktail), and flash frozen in liquid nitrogen. Lysates were subsequently thawed on ice and labelled with 200 pmol of either Cy3 or Cy5 (GE Healthcare, Piscataway, NJ) for 30 min on ice in the dark, according to the manufacturer's protocol, with some modification (Hu *et al.*, 2005). The labelling reaction was quenched with 2 µl of 10 mM lysine for 10 min on ice in the dark. The quenched Cy-labelled samples were then combined and added to an equal volume of 2× rehydration buffer (7 M urea, 2 M thiourea, 4% CHAPS, 4 mg ml⁻¹ DTT) supplemented with 0.5% IPG (Immobilized pH gradient) buffer 3–11. Labelled protein extracts were separated by standard 2D gel electrophoresis using an IPGphor first-dimension isoelectric focusing unit (GE Healthcare) and 24 cm 3–11 immobilized pH gradient strips (GE Healthcare). Isoelectrically focused samples were reduced and alkylated with DTT and iodoacetamide and equilibrated into the second dimension loading buffer (6 M Urea, 30% glycerol, 2% SDS, 50 mM Tris pH 8.8) per manufacturer's protocol. Second-dimension focusing was performed on a 12% SDS-PAGE 24 cm gel using an Ettan DALT 12 unit (GE Healthcare). Gels were pre-cast and pre-silanized (Bind-silane, GE Healthcare) to affix the polymerized gel to one of the two low-fluorescence glass plates. Following second-dimension focusing, the gel was fluorescently scanned using a Typhoon 9400 variable mode imager (GE Healthcare) to detect Cy3- and Cy5-specific emissions corresponding to protein concentration (Tonge *et al.*, 2001; Gharbi *et al.*, 2002). Fluorescent gel images were then analysed using Decyder Differential In-Gel Analysis software (GE Healthcare), where individual spot volume ratios were calculated for each protein spot pair.

Protein identification using tandem mass spectrometry

Gel features were selected in the Decyder software and the (X,Y) co-ordinates were automatically saved in a file for spot excision. Translation from the co-ordinates of the DIA image to the co-ordinates used by the picking robot (ProPic, Genomic Solutions, Ann Arbor, MI) was accomplished using in-house software. The central cores (1.8 mm) of the selected gel features were excised and transferred to a 96 well source plate. The gel pieces were digested *in situ* with trypsin as previously described (Havlis *et al.*, 2003). Aliquots (0.5 µl) were removed and mixed with a matrix solution of α -cyano-hydroxycinnamic acid (0.5 µl, Premix, Agilent, Palo Alto, CA). The peptides were spotted onto a stainless steel target for matrix-assisted laser desorption ionization mass spectrometry (MALDI-MS). Spectra of the peptide pools were obtained on a MALDI-TOF/TOF instrument (ABI 4700) (Medzihradzky *et al.*, 2000) and operated as previously described (Bredemeyer *et al.*, 2004) using peptides from trypsin autolysis ($m/z = 842.51$, 1045.56 and 2211.10) (Harris *et al.*, 2002). The most intense MS signals ($n = 7-20$) were automatically selected for tandem analysis using the MALDI-TOF/TOF instrument after exclusion of observed m/z -values from contaminants. The peptide fragmentation spectra were processed (centroiding and background subtraction) with GPS

Explorer and searched using MASCOT, V1.9 (Matrix Sciences, London) against the most recent NCBI non-redundant database (26-07-2005 build date), which contained the published genome of *E. histolytica*. Carbamidomethylation of cysteine residues, single oxidations of methionine residues were set as the 'variable modifications' in the MASCOT software. The following criteria were used to rule out false positive protein identifications from the MASCOT results: (i) at least two peptides with at least one individual peptide with a MASCOT scores > 50, (ii) observing five sequential intense fragmentation ions that correspond to the peptide sequence and (iii) observed mass measurement accuracy of ± 20 ppm.

Peptide pools from the gel features that were unidentified using MALDI-MS/MS were analysed using capillary reversed-phase HPLC-MS/MS using an electrospray-quadrupole time-of-flight mass spectrometer (Q-STAR XL, Applied Biosystems) interfaced to a low flow (20–200 nl min⁻¹) liquid chromatograph (Eksigent nano-LC, Eksigent, Livermore, CA) as previously described (Bredemeyer *et al.*, 2004). Peptide pools from gel features that remained unidentified by either MALDI-MS/MS or quadrupole-TOF-LC-MS/MS were analysed using nano-LC-linear-quadrupole ion trap Fourier transform ion cyclotron resonance mass spectrometry as previously described (King *et al.*, 2006). Identifying peptide information for the six proteins can be found in Table S1.

Real-time PCR for grainin gene expression analysis

Approximately 200 mg of a human colonic xenograft at 4, 12 or 24 h after infection with 1×10^6 *E. histolytica* HM-1:IMSS trophozoites was obtained and saved in 3 ml RNALater reagent (Ambion, Austin, TX). *E. histolytica* HM-1:IMSS trophozoites (1×10^6) grown in log phase culture served as the source for control *E. histolytica* RNA. RNA was isolated using TRIZOL reagent (Invitrogen, Carlsbad, CA) and purified with RNeasy mini kit (Qiagen, Valencia, CA) according to the manufacturer's instructions. The RNA obtained from four infected human xenografts at each time point was pooled. Reverse transcription was carried out with Invitrogen Superscript III without RNase and Invitrogen oligo dT primers per manufacturer's instructions, then treated with Invitrogen RNase H to degrade remaining RNA. Treated cDNA was diluted and amplified using SYBR Green Master Mix 2x reagent (Applied Biosystems) in an Applied Biosystems 7500 Real-time analyser in a total of 25 µl per reaction run in triplicate, per manufacturer's instructions. Up to four reference gene transcripts were measured from each sample, and were analysed using Excel (Microsoft, Redmon, WA) with the add-in module geNorm (<http://medgen.ugent.be/~jvdesomp/genorm/>) used to normalize amoebic total mRNA abundance between grafts and cultured amoeba (Vandesompele *et al.*, 2002). Graphs were constructed using Microsoft Excel. Primers were designed with, and obtained through, Primer-Quest (<http://www.idtdna.com>) using sequence information from NCBI, and NCBI BLAST was used to confirm primer specificity against the current *Entamoeba* dataset. Primer sequences use for real-time amplification are as follows: 5' PFDR: GGAGCTAATCCAGCTCAAGCATTC; 3' PFDR: GACCAGTATCCACTGTAACTGCC; 5' Histone H3: TCCA GGTGCAGTTGCTCTTACTGA; 3' Histone H3: CTGACAA

GAGCTTGGAAATGGTGTCT; 5' Grainin 1: CACTGCTGCATATCAAGCTGATCC; 3' Grainin 1: GAGGTAGCAAGTGGATACCACCAT; 5' Grainin 2: TCAAGCTGCTGTAACTCTGATCC; 3' Grainin 2: TGGAACCACCATTGGAACCTTGAG; 5' Peroxiredoxin TGTCCACTCAATTGGAACCAGGC; 3' Peroxiredoxin: CCATCTGGTGTGGTTCAATGGTG.

Western blot analysis

To confirm overexpression of peroxiredoxin, total lysates were created from HM-1:IMSS, Rahman and Rahman transfected with pNeoPRD as previously described (Stanley *et al.*, 1995). Lysates were run on a gradient SDS-PAGE gel and transferred to PVDF. A Western blot was performed with 1:1200 rabbit anti-peroxiredoxin antibodies provided by Dr Iris Bruchhaus (Bernard Nocht Institute, Hamburg), followed by HRP-labelled anti-rabbit IgG antibodies. PVDF membrane was then stripped and reprobed with anti-actin antibodies (Chemicon, Temecula, CA). Densitometry was computed with Adobe Photoshop (San Jose, CA).

Confocal immunofluorescence microscopy

Confocal immunofluorescence microscopy was performed as previously described with minor modifications (Choi *et al.*, 2005). Trophozoites were chilled and washed 2× in cold PBS, fixed in formalin for 15 min at room temperature, and blocked with 3% BSA or permeabilized with 0.1% Triton X-100 for 10 min prior to blocking. Polyclonal rabbit anti-peroxiredoxin sera, diluted 1:200 in blocking buffer, were used to stain fixed and blocked trophozoites overnight at 4°C. Cells were washed 2× with cold blocking buffer and 1× with cold PBS. Secondary goat anti-rabbit IgG-Alexa 488 conjugated antibodies (Molecular Probes, Eugene, OR) were diluted 1:500 and added to washed trophozoites at room temperature for 1 h, followed by another washing cycle. Stained amoeba were visualized on a Zeiss LSM510 microscope.

Hydrogen peroxide killing assay

H₂O₂ killing assays were carried out as previously described (Choi *et al.*, 2005). Briefly, strains HM-1, Rahman and R-pNeoPRD were isolated from log-phase culture, chilled and spun at 4°C, 400 g for 5 min. Amoeba were resuspended in DMEM in addition to 70 mg L-cysteine and 135 mg ascorbate per 100 ml to a final concentration of 5 × 10⁵ cells ml⁻¹. Trophozoites were treated with or without 5 mM H₂O₂ (Sigma-Aldrich) at 37°C for 1 h. Trypan blue (Sigma-Aldrich) staining was used to determine amoeba viability.

Acknowledgements

The authors would like to thank the personnel of the Washington University Proteomics Center for their assistance in these studies, and the laboratory of Dr Daniel Goldberg for providing HRBCs. Plasmid pNeoPRD and anti-peroxiredoxin antibodies were graciously donated by Dr Iris Bruchhaus. This work was supported by NIH Grants AI37977 and AI30084 to S.L.S., U54AI057160, the Midwest Regional

Center of Excellence for Biodefense and Emerging Infectious Diseases Research, HD00836 to the Birth Defects Research Laboratory at the University of Washington, P41RF00954 to the Proteomics Center at Washington University, DK25275 to the Digestive Diseases Research Core Center at Washington University, and additional funds provided to the Proteomics Center by Washington University. S.L.S. is a Burroughs Wellcome Scholar in Molecular Parasitology. PHD was supported by Training Grant AI0717225.

References

- Akbar, M.A., Chatterjee, N.S., Sen, P., Debnath, A., Pal, A., Bera, T., and Das, P. (2004) Genes induced by a high-oxygen environment in *Entamoeba histolytica*. *Mol Biochem Parasitol* **133**: 187–196.
- Bredemeyer, A.J., Lewis, R.M., Malone, J.P., Davis, A.E., Gross, J., Townsend, R.R., and Ley, T.J. (2004) A proteomic approach for the discovery of protease substrates. *Proc Natl Acad Sci USA* **101**: 11785–11790.
- Bruchhaus, I., Richter, S., and Tannich, E. (1997) Removal of hydrogen peroxide by the 29 kDa protein of *Entamoeba histolytica*. *Biochem J* **326**: 785–789.
- Bruchhaus, I., Roeder, T., Lotter, H., Schwerdtfeger, M., and Tannich, E. (2002) Differential gene expression in *Entamoeba histolytica* isolated from amoebic liver abscess. *Mol Microbiol* **44**: 1063–1072.
- Bujanover, S., Katz, U., Bracha, R., and Mirelman, D. (2003) A virulence attenuated amoebapore-less mutant of *Entamoeba histolytica* and its interaction with host cells. *Int J Parasitol* **33**: 1655–1663.
- Burchard, G.D., and Mirelman, D. (1988) *Entamoeba histolytica*: virulence potential and sensitivity to metronidazole and emetine of four isolates possessing nonpathogenic zymodemes. *Exp Parasitol* **66**: 231–242.
- Choi, M.H., Sajed, D., Poole, L., Hirata, K., Herdman, S., Torian, B.E., and Reed, S.L. (2005) An unusual surface peroxiredoxin protects invasive *Entamoeba histolytica* from oxidant attack. *Mol Biochem Parasitol* **143**: 80–89.
- Davis, P.H., and Stanley, S.L., Jr. (2003) Breaking the species barrier: use of SCID mouse-human chimeras for the study of human infectious diseases. *Cell Microbiol* **5**: 849–860.
- Diamond, L.S., Harlow, D.R., and Cunnick, C.C. (1978) A new medium for the axenic cultivation of *Entamoeba histolytica* and other *Entamoeba*. *Trans R Soc Trop Med Hyg* **72**: 431–432.
- Dvorak, J.A., Kobayashi, S., Nozaki, T., Takeuchi, T., and Matsubara, C. (2003) Induction of permeability changes and death of vertebrate cells is modulated by the virulence of *Entamoeba* spp. isolates. *Parasitol Int* **52**: 169–173.
- Gharbi, S., Gaffney, P., Yang, A., Zvelebil, M.J., Cramer, R., Waterfield, M.D., and Timms, J.F. (2002) Evaluation of two-dimensional differential gel electrophoresis for proteomic expression analysis of a model breast cancer cell system. *Mol Cell Proteomics* **1**: 91–98.
- Gilchrist, C.A., Houpt, E., Trapaidze, N., Fei, Z., Crasta, O., Asgharpour, A., *et al.* (2006) Impact of intestinal colonization and invasion on the *Entamoeba histolytica* transcriptome. *Mol Biochem Parasitol* **147**: 163–176.
- Hamann, L., Nickel, R., and Tannich, E. (1995) Transfection and continuous expression of heterologous genes in the

- protozoan parasite *Entamoeba histolytica*. *Proc Natl Acad Sci USA* **92**: 8975–8979.
- Harris, W.A., Janecki, D.J., and Reilly, J.P. (2002) Use of matrix clusters and trypsin autolysis fragments as mass calibrants in matrix-assisted laser desorption/ionization time-of-flight mass spectrometry. *Rapid Commun Mass Spectrom* **16**: 1714–1722.
- Havlis, J., Thomas, H., Sebela, M., and Shevchenko, A. (2003) Fast-response proteomics by accelerated in-gel digestion of proteins. *Anal Chem* **75**: 1300–1306.
- Hu, X., Friedman, D., Hill, S., Caprioli, R., Nicholson, W., Powers, A.C., et al. (2005) Proteomic exploration of pancreatic islets in mice null for the alpha2A adrenergic receptor. *J Mol Endocrinol* **35**: 73–88.
- Kadmas, J.L., and Beckerle, M.C. (2004) The LIM domain: from the cytoskeleton to the nucleus. *Nat Rev Mol Cell Biol* **5**: 920–931.
- King, J.B., Gross, J., Lovly, C.M., Rohrs, H., Piwnicka-Worms, H., and Townsend, R.R. (2006) Accurate mass-driven analysis for the characterization of protein phosphorylation. Study of the human chk2 protein kinase. *Anal Chem* **78**: 2171–2181.
- Lauwaet, T., Oliveira, M.J., De Callewaert, B.B.G., Mareel, M., and Leroy, A. (2004) Proteinase inhibitors TPCCK and TLCK prevent *Entamoeba histolytica* induced disturbance of tight junctions and microvilli in enteric cell layers in vitro. *Int J Parasitol* **34**: 785–794.
- Leroy, A., Lauwaet, T., De Oliveira, M.B.G., Bracha, R., Ankri, S., et al. (2000) Disturbance of tight junctions by *Entamoeba histolytica*: resistant vertebrate cell types and incompetent trophozoites. *Arch Med Res* **31**: S218–S220.
- Li, E., Becker, A., and Stanley, S.L., Jr. (1988) Use of Chinese hamster ovary cells with altered glycosylation patterns to define the carbohydrate specificity of *Entamoeba histolytica* adhesion. *J Exp Med* **167**: 1725–1730.
- MacFarlane, R.C., and Singh, U. (2006) Identification of differentially expressed genes in virulent and nonvirulent *Entamoeba* species: potential implications for amebic pathogenesis. *Infect Immun* **74**: 340–351.
- Marion, S., Wilhelm, C., Voigt, H., Bacri, J.C., and Guillen, N. (2004) Overexpression of myosin IB in living *Entamoeba histolytica* enhances cytoplasm viscosity and reduces phagocytosis. *J Cell Sci* **117**: 3271–3279.
- Mattern, C.F., Keister, D.B., and Caspar, P.A. (1978) Experimental amebiasis. III. A rapid in vitro assay for virulence of *Entamoeba histolytica*. *Am J Trop Med Hyg* **27**: 882–887.
- Medzihradsky, K.F., Campbell, J.M., Baldwin, M.A., Falick, A.M., Juhasz, P., Vestal, M.L., and Burlingame, A.L. (2000) The characteristics of peptide collision-induced dissociation using a high-performance MALDI-TOF/TOF tandem mass spectrometer. *Anal Chem* **72**: 552–558.
- Moody, S., Becker, S., Nuchamowitz, Y., and Mirelman, D. (1998) Identification of significant variation in the composition of lipophosphoglycan-like molecules of *E. histolytica* and *E. dispar*. *J Eukaryot Microbiol* **45**: 9S–12S.
- Moody-Haupt, S., Patterson, J.H., Mirelman, D., and McConville, M.J. (2000) The major surface antigens of *Entamoeba histolytica* trophozoites are GPI-anchored proteophosphoglycans. *J Mol Biol* **297**: 409–420.
- Nickel, R., Jacobs, T., Urban, B., Scholze, H., Bruhn, H., and Leippe, M. (2000) Two novel calcium-binding proteins from cytoplasmic granules of the protozoan parasite *Entamoeba histolytica*. *FEBS Lett* **486**: 112–116.
- Orozco, E., Suarez, M.E., and Sanchez, T. (1985) Differences in adhesion, phagocytosis and virulence of clones from *Entamoeba histolytica*, strain HM1:IMSS. *Int J Parasitol* **15**: 655–660.
- Rodriguez, M.A., and Orozco, E. (1986) Isolation and characterization of phagocytosis- and virulence-deficient mutants of *Entamoeba histolytica*. *J Infect Dis* **154**: 27–32.
- Samarawickrema, N.A., Brown, D.M., Upcroft, J.A., Thammapalerd, N., and Upcroft, P. (1997) Involvement of superoxide dismutase and pyruvate: ferredoxin oxidoreductase in mechanisms of metronidazole resistance in *Entamoeba histolytica*. *J Antimicrob Chemother* **40**: 833–840.
- Seydel, K.B., Li, E., Swanson, P.E., and Stanley, S.L., Jr. (1997) Human intestinal epithelial cells produce proinflammatory cytokines in response to infection in a SCID mouse-human intestinal xenograft model of amebiasis. *Infect Immun* **65**: 1631–1639.
- Seydel, K.B., Li, E., Zhang, Z., and Stanley, S.L., Jr. (1998) Epithelial cell-initiated inflammation plays a crucial role in early tissue damage in amebic infection of human intestine. *Gastroenterology* **115**: 1446–1453.
- Som, I., Azam, A., Bhattacharya, A., and Bhattacharya, S. (2000) Inter- and intra-strain variation in the 5.8S ribosomal RNA and internal transcribed spacer sequences of *Entamoeba histolytica* and comparison with *Entamoeba dispar*, *Entamoeba moshkovskii* and *Entamoeba invadens*. *Int J Parasitol* **30**: 723–728.
- Stanley, S.L., Jr. (2003) Amoebiasis. *Lancet* **361**: 1025–1034.
- Stanley, S.L., Jr, Tian, K., Koester, J.P., and Li, E. (1995) The serine-rich *Entamoeba histolytica* protein is a phosphorylated membrane protein containing O-linked terminal N-acetylglucosamine residues. *J Biol Chem* **270**: 4121–4126.
- Tonge, R., Shaw, J., Middleton, B., Rowlinson, R., Rayner, S., Young, J., et al. (2001) Validation and development of fluorescence two-dimensional differential gel electrophoresis proteomics technology. *Proteomics* **1**: 377–396.
- Vandesompele, J., De, P.K., Pattyn, F., Poppe, B., Van, R.N., De, P.A., and Speleman, F. (2002) Accurate normalization of real-time quantitative RT-PCR data by geometric averaging of multiple internal control genes. *Genome Biol* **3**: RESEARCH0034.
- Wassmann, C., Hellberg, A., Tannich, E., and Bruchhaus, I. (1999) Metronidazole resistance in the protozoan parasite *Entamoeba histolytica* is associated with increased expression of iron-containing superoxide dismutase and peroxiredoxin and decreased expression of ferredoxin 1 and flavin reductase. *J Biol Chem* **274**: 26051–26056.

Supplementary material

The following supplementary material is available for this article online:

Table S1. Identifying peptide information for six differentially expressed proteins. Mascot software calculations of protein identity were obtained from mass spectrometric analysis. Identifying peptides are highlighted within the full protein sequence, and are delineated below each sequence.

This material is available as part of the online article from <http://www.blackwell-synergy.com>